JOURNAL OF SPACECRAFT AND ROCKETS
Vol. 41, No. 4, July–August 2004

North Star Plasma-Jet Experiment Particles and Electric and Magnetic Field Measurements

B. G. Gavrilov,* I. M. Podgorny,† D. B. Sobyanin,‡ and J. I. Zetzer§
Russian Academy of Sciences, 117334, Moscow, Russia
R. E. Erlandson¶ and C. I. Meng**
Johns Hopkins University, Applied Physics Laboratory, Laurel, Maryland 20723-6099
R. F. Pfaff††
NASA Goddard Space Flight Center, Greenbelt, Maryland 20771
and
K. A. Lynch‡‡
New Hampshire University, Durham, New Hampshire 03824

The results of measurements of magnetic and electric fields, plasma ions energy, and plasma density during the Russian–American North Star active experiment are presented. The experiment was carried out in the auroral ionosphere on 22 January 1999. A Black Brant XII rocket, having two explosive aluminum plasma generators plus scientific payloads onboard, was launched at 13:57:03 UT from Poker Flat, Alaska. Two plasma-jet injections across the magnetic field were made at the altitudes 280 and 360 km, respectively. Before injection 1, an air cloud was released to increase jet ionization. At injection 1, the maximum plasma density exceeded the density at injection 2 by two orders of magnitude. This can be explained by charge stripping of aluminum atoms when the jet propagated through the dense air cloud. Only at injection 1 was complete expelling of the magnetic field by the plasma jet observed. A weak plasma deceleration was indicated by magnetic field compression before the jet front. At injection 2, the magnetic field was weakened only by 1%. A polarization electric field $E = -V \times B$ generated field-aligned currents, which involved the ionospheric plasma in motion, and the plasma jet efficiently decelerated.

Nomenclature

B	=	magnetic field, nT
E	=	electric field, V/cm
E_x, E_y, E_z	=	electric field components in the payload reference frame, V/cm
l_p	=	length of cylindrical Langmuir probe, mm
m_i	=	ion mass, amu
n_i	=	plasma density, cm^{-3}
r_p	=	radius of cylindrical Langmuir probe, mm
V	=	plasma velocity, km/s
V_A	=	Alfvén velocity, km/s
V_p	=	bias of Langmuir probe, V
δB_x, δB_y, δB_z	=	variation of magnetic field components in the payload reference frame, nT

Received 19 October 2001; revision received 21 January 2003; accepted for publication 17 July 2003.

*Head of Laboratory of the Magnetosphere-Earth Coupling, Institute of Geospheres Dynamics, 38 Leninsky Prospect, Building 1; gavrilov@idg.chph.ras.ru.

†Senior Scientist, Laboratory of the Magnetosphere-Earth Coupling, Institute of Geospheres Dynamics, 38 Leninsky Prospect, Building 1.

‡Research Scientist, Laboratory of the Magnetosphere-Earth Coupling, Institute of Geospheres Dynamics, 38 Leninsky Prospect, Building 1; sobyanin@idg.chph.ras.ru.

§Deputy Director, Institute of Geospheres Dynamics, 38 Leninsky Prospect, Building 1; zertzer@idg.chph.ras.ru.

¶Assistant Group Supervisor, Space Department, 11100 Johns Hopkins Road; erlandson@jhuapl.edu.

**Branch Supervisor, Space Department, 11100 Johns Hopkins Road; ching.meng@jhuapl.edu.

††Senior Scientist, Code 696; rob.pfaff@gsfc.nasa.gov.

‡‡Senior Scientist, Dartmouth College; lynch@birkeland.Dartmouth.edu.

Introduction

MANY important phenomena in space physics are associated with high-density plasma-jet interaction with an ambient magnetized plasma, and the investigation of the artificial plasma jet interactions with the magnetic field in active experiments in the magnetosphere is very important.[1] However, plasma-jet dynamics, jet deceleration, and magnetohydrodynamic wave generation still remained a topic of discussion. Earlier we reported an investigation of plasma-jet propagation along the geomagnetic field in the Fluxus rocket experiments,[2,3] where a chemical explosive generator was used for plasma-jet creation. During Fluxus, a diamagnetic cavity was observed ~100 m from the plasma jet source, with a jet velocity reaching 45 km/s and a plasma density $\sim 10^9$ cm^{-3}. In this paper, we present some results of the new Russian–American North Star active experiment with jet injection across the magnetic field.

The main goal of the North Star experiment[4,5] is to investigate the influence of the background density and geomagnetic field on plasma-jet dynamics and environmental phenomena accompanying plasma propagation. Two aluminum plasma injections were carried out across the geomagnetic field. Special explosive generators that produce a high-velocity dense aluminum plasma jet were used.[5] Three separate scientific payloads allowed us to obtain data on plasma-jet evolution in the ionosphere from the time of injection essentially up to the loss of jet energy.

This paper is devoted to description and preliminary analysis of particle, electric field, and magnetic field measurements during the North Star experiment. Before performing this space experiment, we simulated a jet interaction with ambient plasma and perpendicular magnetic field in numerical[6,7] and laboratory[8,9] experiments. These experiments showed the magnetic field increasing ahead of the magnetic cavity and jet deceleration caused by field-aligned current generation. These results were taken into consideration in the design of a scenario for the North Star experiment and in the choice of probe parameters.

Plasma density and magnetic field measurements were executed by the Institute of Geospheres Dynamics, the Johns Hopkins University, Applied Physics Laboratory, and NASA's Goddard Space

Flight Center (GSFC). Electric field measurements were carried out by GSFC.[5] Particle fluxes were investigated using the University of New Hampshire electrostatic analyzers.[5,10]

Experiment

The North Star experiment was carried out on 22 January 1999 in the auroral ionosphere. A Black Brant XII sounding rocket having two explosive-type generators (ETG-1 and ETG-2), a plasma diagnostic payload (PDP), and an optical sensors payload (OSP) was launched at 1357:03 UT from Poker Flat, Alaska, in the northerly direction. The payloads were situated on a line so that the plasma jet would pass each payload consecutively.

In the experiment, two plasma injections across the magnetic field were carried out at the altitudes 280 and 360 km, respectively. The first injection (injection 1) was produced at 1402:48 UT by the plasma explosive generator installed on ETG-1. The measurements of plasma density and magnetic field were carried out by the probes on ETG-2, PDP, and OSP at the distances of 170, 468, and 1020 m, respectively (Fig. 1a). The electric field and particle fluxes were registered on the PDP. The second injection (injection 2) was made at 1405:23 by ETG-2, and the measurements were carried out only on PDP and OSP at distances of about 537 and 1595 m, respectively (Fig. 1b). The main difference between the two injections was that about 7 g of compressed air was released 0.2 s before injection 1 was detonated. The purpose of creating the air cloud was to increase jet ionization through interaction of the jet with the neutral particles of air. Injection 2 took place without release of an air cloud.

The ion density was measured by Langmuir probes. On the ETG-2 and PDP, cylindrical probes of stainless steel were used. In addition, a spherical Langmuir probe was located on one of the 5-m boom (not discussed here). The cylindrical probes were installed on short folding isolated booms on the front plate of the payloads. On the ETG-2, two Langmuir-probe sensors were used (radii and lengths $r_p = 0.5$ mm, $l_p = 30$ mm and $r_p = 3$ mm, $l_p = 100$ mm). The onboard system supplied measurements of ion density in the range of 10^5 to 5×10^9 cm^{-3} in the bandwidth 1–100,000 Hz and in the range of 5×10^9 to 5×10^{12} cm^{-3} in the bandwidth 1–50,000 Hz. PDP also had two Langmuir-probe sensors ($r_p = 0.5$ mm, $l_p = 50$ mm and $r_p = 5$ mm, $l_p = 100$ mm). The measurements were carried out in the range of 10^4–10^8 cm^{-3} in the bandwidth 1–50,000 Hz and in the range of 10^8–10^{11} cm^{-3} in bandwidth 1–10,000 Hz. The probes worked in a fixed-bias mode ($V_p = -10$ V) and collected ion saturation current. It is assumed that the gauges were directed along the stream movement, so that the influence of plasma velocity on the probe current was not taken into account. Ion density was estimated using formulas for an orbital-motion-limited case. In calculations the temperature of the plasma was assumed to be 10^4 K (Ref. 11). During injection 2, PDP was inclined at an angle of about 80 deg to the direction of jet propagation, so that the dependence of probe current on the jet velocity was taken into account. On the OSP, ion density measurements in the bandwidth 0–3 kHz were produced by a flat probe operating in fixed-bias mode. The probe sensor was a circular disk of 3.8-cm diam, surrounded by a guard. Ion density in the jet was calculated assuming that ions move to the probe with a time-of-flight velocity.

A three-axis search coil high-speed magnetometer was used for magnetic field registration on ETG-2 and PDP in the bandwidth 0.3–50,000 Hz. Resolution is about 50 nT. The probe was installed on a folding dielectric boom. Magnetic field measurements on OSP were carried out by a three-axis fluxgate magnetometer in the bandwidth 0–4500 Hz. Resolution is about 2 nT. All magnetic field data presented in the following sections of this paper are given in the payload reference frame. The B_x, B_y components are in the spin plane. The B_z component is along the payload spin axis, which corresponds to the direction of the jet propagation in the case of injection 1.

Electric field measurements were produced by the probe on PDP, which consisted of three sets of extendable dipole antennas, 6 m in length from tip to tip.[5] A spherical sensor of 6.35 cm diam was mounted at the end of each electric field boom. Electric fields shown in this paper are in the payload reference frame. The E_x and E_y data are in the spin plane. The E_z data are along the spin axis of the payload. Accuracy of electric field measurement in the range of 0–20 kHz is about 1 mV/m.

Ion fluxes were measured by a top-hat hemispherical electrostatic analyzer[5,10] that registers ions in the range of 10–400 eV. The energy sweep had 16 steps of 0.4-ms duration each. The aperture plane was parallel to the spin axes of the payload.

Results of Measurements

An initial peak in the high-gain Langmuir-probe signals was detected at the beginning of both detonations. This signal is explained by photoemission from the probe surface because of ultraviolet radiation at the initial phase of the injection. Hereafter the initial peak of the probe signals is taken as the time of the detonation; therefore, the time in all figures is referenced to the time of plasma injections.

Injection 1

The results of measurements at ETG-2 are shown in Fig. 2. Significant growth of the plasma density n_i is detected at a 170-m distance 4 ms after injection. This growth corresponds to a plasma velocity of 42 km/s. At the jet front, high-frequency fluctuations of the probe current are registered (Fig. 2 at 4 ms). The maximum plasma density $n_i = 3 \times 10^9$ cm^{-3} is detected at 7 ms. The plasma density exceeds the ambient level for 250 ms.

For technical reasons, only one component of the magnetic field was registered on ETG-2. A smooth increase of the magnetic field is seen at 1 ms. At 5 ms a sharp decrease of the magnetic field is observed, which is evidence of a diamagnetic cavity appearing. This time corresponds to a jet velocity of 34 km/s. The maximum field deviation is $\sim 8 \times 10^3$ nT.

The experimental results obtained at PDP are shown in Fig. 3. A sharp increase in plasma density on PDP is detected 14 ms after injection. This time corresponds to a jet velocity of 33 km/s at the distance from ETG-2 to PDP. High-frequency fluctuations at the front of the plasma jet are also seen. The maximum plasma density $n_i = 3 \times 10^9$ cm^{-3} is observed at 18 ms. Plasma density greatly exceeding the background densities is observed for 400 ms.

A gradual increase of the magnetic field is revealed at 9–10 ms after injection. This increase can be explained by the arrival of a magnetosonic wave. At 17–18 ms, a sharp decrease of the magnetic field signal was registered for all three components; this indicates the onset of a diamagnetic effect. The diamagnetic cavity propagates with a velocity of about 27.5 km/s. The maximum field perturbation reaches about 5×10^4 nT. Thus the signal from PDP

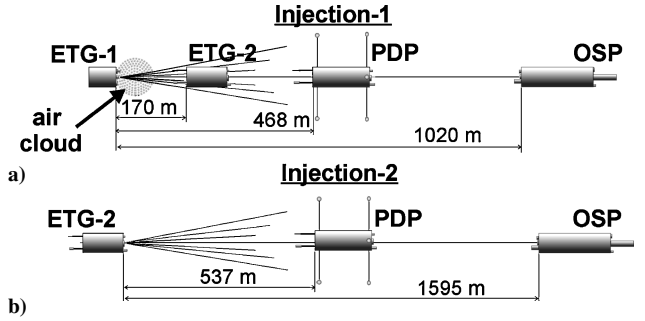

Fig. 1 Payload positions injections 1 and 2.

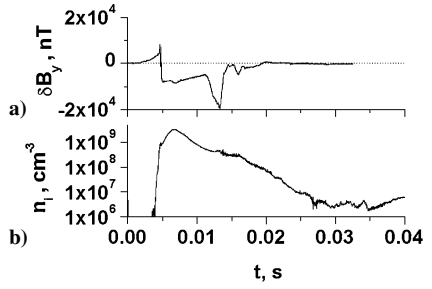

Fig. 2 Injection 1, explosive-type generator-2 (ETG-2) payload. One component of the a) magnetic field and b) ion density.

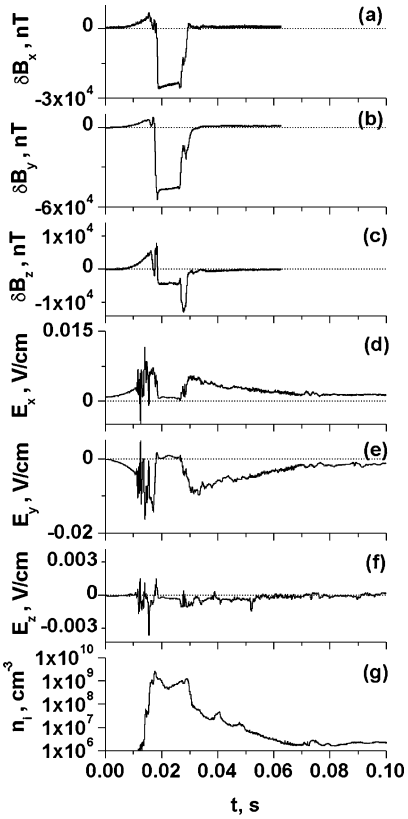

Fig. 3 Injection 1, plasma diagnostic payload: a–c) three components of the magnetic field, d–f) three components of the electric field, and g) ion density.

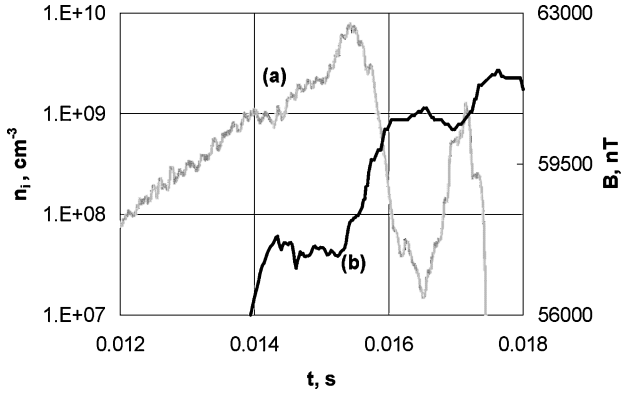

Fig. 4 Injection 1, PDP: leading edge of the diamagnetic cavity (curve a) and the ion density (curve b).

demonstrates a complete expelling of the magnetic field from the plasma jet. One can see also that the diamagnetic signal duration coincides with the most dense part of the plasma arriving at the payload ($n_i > 5 \times 10^8$ cm^{-3}). Estimating the ion density at the border of the diamagnetic cavity from the balance of plasma and magnetic field pressure at $T \sim 10^4$ K[11] gives the value of about 10^9 cm^{-3}, which agrees with the measurement results.

Figure 4 shows the leading edge of the diamagnetic cavity from the magnetometer data (curve a) and the Langmuir-probe data (curve b) on PDP. It can be seen that the Langmuir probe registers two peaks of density at 14.5 and 16 ms, which are associated with a corresponding decrease in the local magnetic field. This effect can be explained by plasma front stratification. Each dense layer of plasma reduces the magnetic field according to the value of its ion density.

The electric field data obtained at PDP are shown in the Figs. 3d–3f. A smooth increase of the electric field at the initial part of the

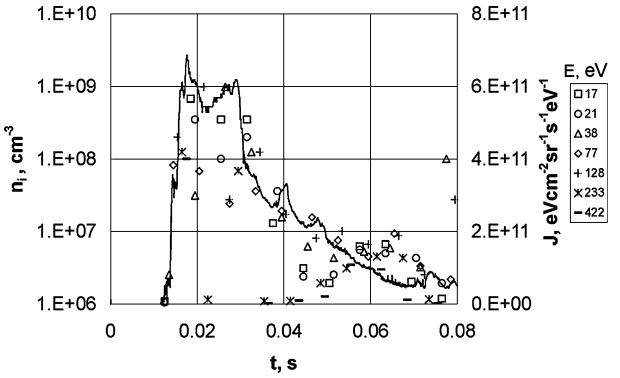

Fig. 5 Injection 1, PDP: ——, ion density and △, □, +, ⁎, ion fluxes in the energy range of 10–422 eV.

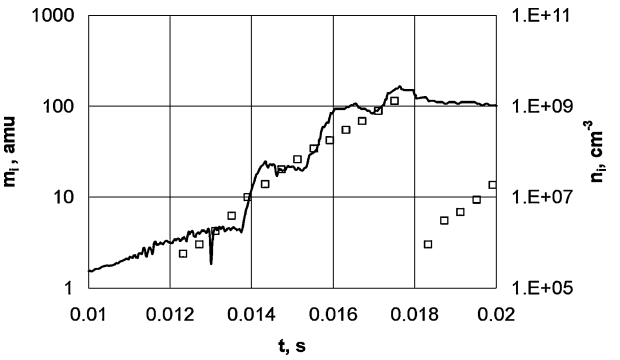

Fig. 6 Injection 1, PDP: ——, ion density and □, estimates of particle masses.

signal is revealed. This increase is also connected to the magnetosonic wave arrival. At ∼10 ms high, frequent fluctuations appear. The maximum total electric field reaches about 0.016 V/cm at 17 ms. This field is connected with background plasma moving in the magnetosonic wave. Then the electric field quickly decreases to zero, which corresponds to the appearance of the diamagnetic cavity. In the region where the magnetic field begins to be restored (∼27 ms), the polarization electric field connected with the plasma moving through the transverse magnetic field also increases. The maximum amplitude of the electric field in this region is 0.01 V/cm. At a magnetic field equal to 5×10^4 nT, this corresponds to a plasma velocity $E/B \sim 20$ km/s. This value is very close to the average jet velocity registered at this time. Further, the total electric field gradually diminishes with the decreasing plasma velocity.

Figure 5 shows the ion density at the PDP distance of 468 m and fluxes of ions with energies in the range of 10–400 eV registered by the electrostatic analyzer in the direction of jet propagation. Figure 6 shows the results of ion mass estimation, calculated from ion energy and time-of-flight velocity, in comparison with ion density data. We can see that the front of the jet coincides with the arrival of particles with average mass corresponding to that of aluminum. At the same time, if we use this method of ion mass estimation we could conclude that at the front of the jet there are particles with apparent mass from several units up to several hundred units mass of a proton. The possible explanation of this effect is that some number of particles arrive with different speeds, and among the ions registered some have lost their energy on the border of the diamagnetic cavity. Also, we cannot exclude the possibility that some ionospheric ions, for example, oxygen, can be entrained by the jet.

The magnetic field and the ion density measured at OSP are shown in Fig. 7. At 55 ms the diamagnetic cavity is seen that corresponds to the ion density increase. The value of the magnetic field decreases by 40%. The peak value of ion density is about 4×10^8 cm^{-3}. The velocity of the plasma jet at the distance between PDP and OSP is 20 km/s. Also, the local peaks of ion density and corresponding decrease in the magnetic field are observed at the front of the jet.

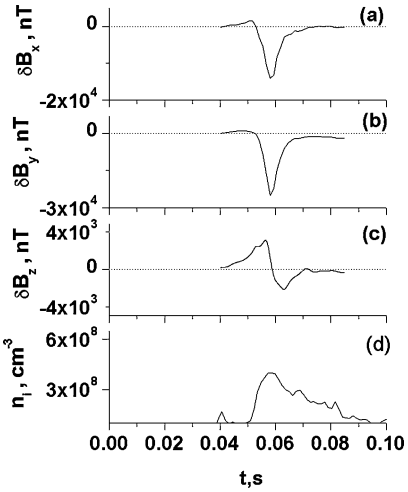

Fig. 7 Injection 1, optical sensors payload: a–c) three components of the magnetic field and d) ion density.

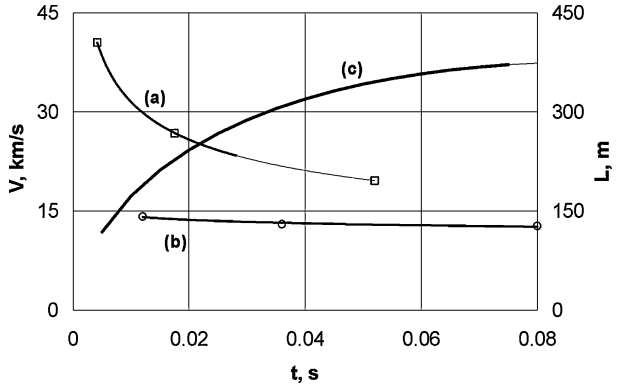

Fig. 8 Injection 1: velocity of the leading edge (curve a) and the trailing edge (curve b) of the diamagnetic cavity and the diamagnetic cavity length (curve c).

The data on the magnetic field variation at 170, 468, and 1020 m permit us to estimate a size for the diamagnetic cavity (Fig. 8), whose borders are assumed to be where the magnetic field decreases by 10%. During cavity propagation, the velocity of the cavity's leading edge (curve a) changes from 42 to about 18 km/s. At the same time the velocity of the trailing edge (curve b) is practically constant at 14 km/s. So the length of the diamagnetic cavity (curve c) grows from ∼100 m at ETG-2 to about 350 m in the region of OSP.

The plasma deceleration in the later stage is a result of field-aligned currents generation. The evidence for these currents appearing is the bipolar parallel electric field at the leading edge of the cavity.[12]

The Langmuir probes' registration of the initial UV splash demands that we consider the question of UV influence on probe signals as a whole. Figure 9a shows the UV radiation power (curve 1) and Langmuir-probe signal (curve 2) at ETG-2. The UV radiation power data are obtained by recalculation of OSP photometer data with the assumption that the UV source approaches the payload with the jet front velocity. The patterns of the curves are similar. Thus we think that UV radiation contributes a certain amount to measurements of ion density. The same situation occurs on PDP (Fig. 9b).

Injection 2

Magnetic and electric fields and ion density in the plasma jet at injection 2 at a distance of 532 m from the injector are shown in Fig. 10. The sharp increase of the plasma density is detected 16 ms after injection and corresponds to a jet velocity of 33.5 km/s. The maximum plasma density is about 4×10^7 cm^{-3}. The plasma density exceeds the ambient level for 400 ms.

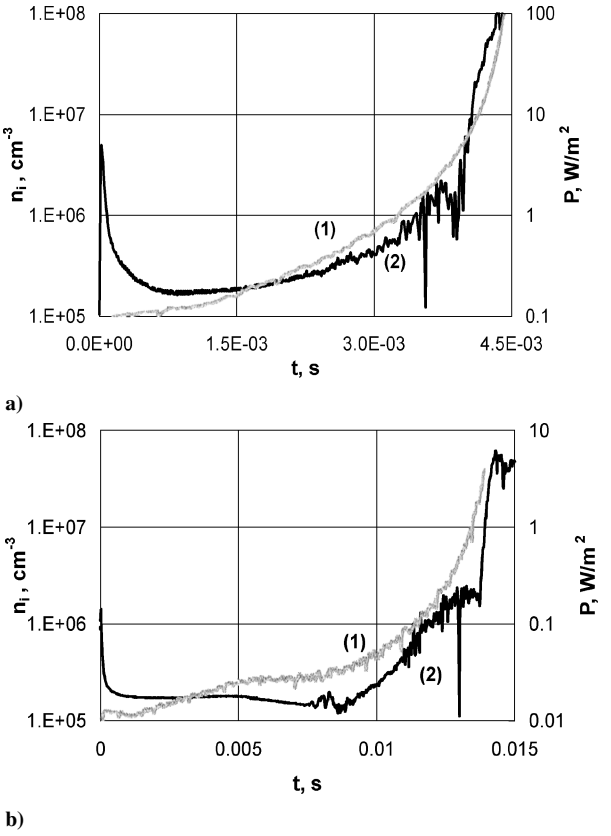

Fig. 9 Injection 1: plasma-jet radiation (curve 1) and ion density (curve 2) on a) ETG-2 and b) PDP.

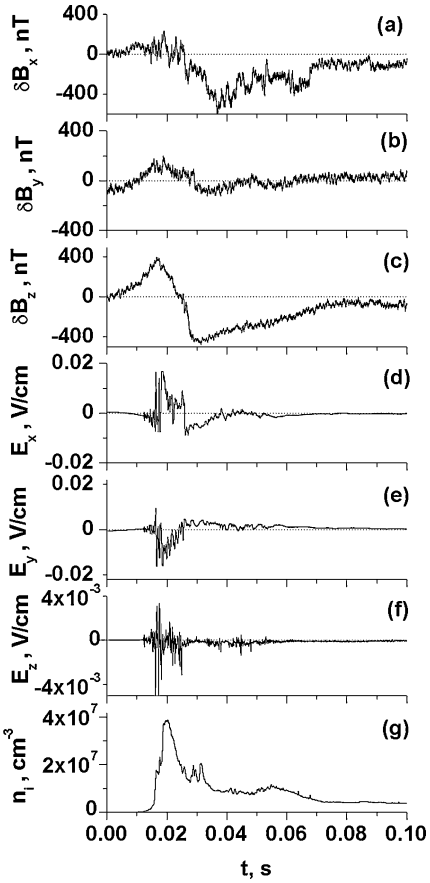

Fig. 10 Injection 2, PDP: a–c) three components of the magnetic field perturbations, d–f) three components of the electric field, and g) the ion density.

The magnetometer shows weak magnetic field perturbation of no more than 10^4 nT. This result can be explained by the smaller ion density of injection 2 compared with injection 1. Indeed, the lowest value for a plasma density that can expel the magnetic field can be determined from the balance of plasma pressure and magnetic field pressure $n_i = (B_0^2 - B_i^2)/8\pi$ kT. Here, B_0 is the local undisturbed geomagnetic field, and B_i is the magnetic field inside the plasma cloud. To expel the magnetic field, the plasma density should be more than 10^8–10^9 cm^{-3} for the typical chemical release temperature 5000–50,000 K. At injection 2 the maximum plasma density measured at PDP is about 4×10^7 cm^{-3}. Such plasma can weaken the magnetic field by no more than 1%, as is observed in the experiment. The magnetic field data registered the frequencies of 29, 48, and 760 Hz, which could be identified as cyclotron frequencies for aluminum, oxygen, and hydrogen. The frequencies of 7.3×10^3 Hz could be related to low-hybrid frequencies.

The electric and magnetic fields gradually increase before the plasma-jet front. This shows that magnetic disturbances are generated at the jet interaction with the ionospheric medium, and these disturbances are propagating ahead of the front across the magnetic field. Such disturbances are magnetosonic waves that propagate with Alfvén velocity across the magnetic field. The magnetosonic waves are similar to ordinary sound waves, but their propagation is determined by magnetic pressure. One can see high-frequency fluctuations of the electric field during the passage of the dense plasma. The peak value of the total electric field is about 0.025 V/cm. A polarization electric field caused by the plasma propagation across the magnetic field is observed 25 ms after the jet injection. The maximum value of the total electric field in that region is about 0.01 V/cm. At a magnetic field of 5000 nT, it corresponds to the plasma velocity $E/B \sim 20$ km/s. This value is very close to the time-of-flight velocity at this time. The total polarization electric field gradually decreases because of diminishing plasma velocity.

Ion fluxes with particle energies in the range of 10–400 eV and plasma density measured at PDP are shown in Fig. 11. Ion density

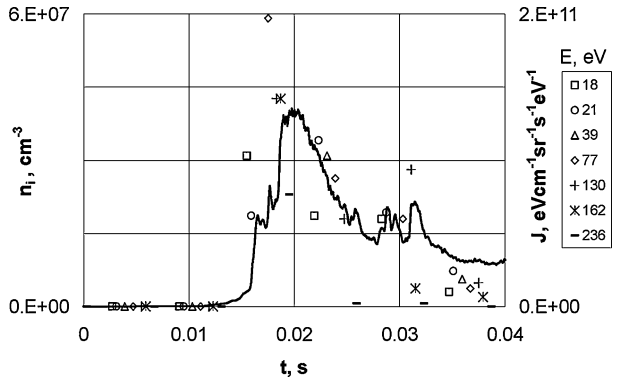

Fig. 11 Injection 2, PDP: ——, ion density and □, △, +, ✳, the ion fluxes in the energy range of 10–422 eV.

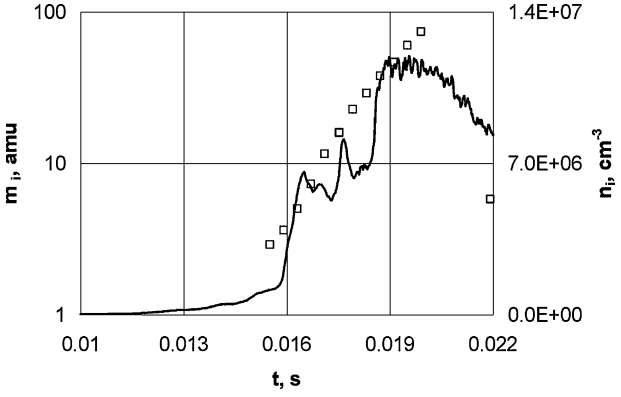

Fig. 12 Injection 2, PDP: ——, ion density and □, estimates of particle masses.

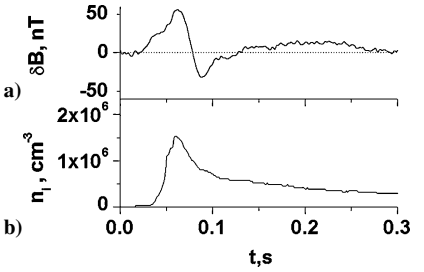

Fig. 13 Injection 2, OSP: a) magnetic field perturbation and the b) ion density.

and estimates of ion mass from ion energy and time-of-flight velocity are displayed in Fig. 12. One can see that fluxes of ions with average mass corresponding to that of aluminum are registered at the front of the plasma. As with injection 1, the registration of ions with mass different from that of aluminum can be explained by the fact that ion velocity differs from time-of-flight velocity.

Figure 13 shows the ion density and the magnetic field perturbations at OSP. The Langmuir probe registers peak ion density at ~60 ms after injection. Magnetic field perturbations are very weak.

Conclusions

The picture of plasma jet evolution looks as follows. After injection 1, the magnetometer registers growth of a weak magnetic field ahead of the plasma-jet arrival. Later the plasma density and the magnetic field increase. This field growth is produced by plasma compression together with the frozen-in magnetic field at plasma deceleration and magnetosonic wave generation. Then the magnetic field decreases, which corresponds to the appearance of a diamagnetic cavity.

The electric field is observed both before and behind the diamagnetic cavity. The first splash of electric field and increase of the magnetic field are also connected with the magnetosonic wave arrival. The increase of the magnetic field δB is the characteristic of the wave power. It is determined by the interaction of the jet front with the magnetized ionospheric plasma. In the magnetosonic wave $\delta V/V_A = \delta B/B$. The wave propagates with velocity V_A. The amplitude of the plasma velocity in the wave is δV. At the trailing edge the electric field appears as a result of propagation of plasma across the magnetic field.

The local maxima of the plasma density and the magnetic field depletion are seen at the leading and trailing edges of the jet. These phenomena are associated with the beginning of plasma stratification. This instability can be developed at the resonance between drift and cyclotron waves.

The probe measurements show that at injection 1 the maximum plasma density exceeds the density at injection 2 by two orders of magnitude, in spite of the fact that the plasma generators were identical for both injections. The production of such dense plasma at injection 1 can be explained by aluminum atom stripping during propagation of the jet through the dense air cloud. On the other hand, the air cloud does not result in substantial loss of kinetic energy by the jet. The data obtained show that the average jet velocity at a distance of about 500 m from the source is comparable for both injections. These velocities are 27.5 and 29 km/s. From this it appears that the amount of neutral air is enough to increase plasma ionization, but it is not enough to cause jet deceleration in the first 500 m.

Only at injection 1 did we observe complete expelling of the magnetic field by the plasma jet. The minimum value of plasma density that can expel the magnetic field can be derived from the balance of magnetic and plasma pressures on the border of a diamagnetic cavity: this value is about 10^8 cm^{-3}. For injection 2 at the distance of about 500 m the maximum ion density was approximately 4×10^7 cm^{-3}, and the magnetic field was weakened by only 1%.

The total expulsion of the magnetic field at the injection 1 provides an electric field $\boldsymbol{E} = -\boldsymbol{V} \times \boldsymbol{B} = 0$. Therefore, field-aligned currents are not induced, and the $\boldsymbol{j} \times \boldsymbol{B}$ force inside the jet is zero. In that case a weak deceleration of the dense plasma is determined only by magnetic field compression before the jet front.

The polarization electric field appears as a result of magnetic field penetration into plasma. The field-aligned currents involve the ionospheric plasma in the motion, and the plasma should be decelerated at a distance of several hundreds meters.

The weak plasma deceleration at a distance of about 500 m from the injector can be explained by the presence of a great deal of highly dense neutral gas in the jet. Indeed, the comparison of the Langmuir probe and pyroprobe data at injection 1 shows that the total (ambient + ion) jet density is more than the ion density by one or two orders of magnitude.[5] The neutrals push the ions by viscosity. In this case the jet dynamics are determined by inertia not of ionized gas but of neutral gas. Later, when an ion-free path grows the neutrals do not affect plasma dynamics. This is the stage of plasma deceleration as a result of field-aligned current generation.

Acknowledgments

The authors thank the sponsors of this project. We also thank the scientists from the Institute of Geospheres Dynamics; Applied Physics Laboratory; NASA Goddard Space Flight Center; Geophysical Institute, University of Alaska Fairbanks; and University of New Hampshire and for participating in the experiment and obtaining and processing data.

References

[1]Brenning, N., "Review of the CIV Phenomenon," *Space Science Reviews*, Vol. 59, Nos. 3–4, 1992, pp. 209–314.

[2]Gavrilov, B. G., Podgorny, A. I., Podgorny, I. M., Sobyanin, D. B., Zetzer, J. I., Erlandson, R. E., Meng, C. I., and Stoyanov, B. J., "Diamagnetic Effect Produced by the Fluxus-1 and -2 Artificial Plasma Jet," *Geophysical Research Letters*, Vol. 26, No. 11, 1999, pp. 1549–1552.

[3]Gavrilov, B. G., Podgorny, I. M., Sobyanin, D. B., Baryshev, V. I., Dvoeglasov, Yu. B., and Podgorny, A. I., "Plasma Jet Interaction with the Geomagnetic Field in Geophysical Fluxus-1 and Fluxus-2 Experiments," *Cosmic Research*, Vol. 38, No. 3, 2000, pp. 229–238.

[4]Gavrilov, B. G., Zetzer, J. I., Podgorny, I. M., Sobyanin, D. B., Meng, C. I., Erlandson, R. E., Stenbaek-Nielsen, H. C., Pfaff, R. F., and Lynch, K. A., "Plasma Jet Motion Across the Geomagnetic Field in 'North Star' Active Geophysical Experiment," *Cosmic Research*, Vol. 41, No. 1, 2003, pp. 28–38.

[5]Erlandson, R. E., Meng, C. I., Zetzer, J. I., Kiselev, Y., Gavrilov, B. G., Stenbaek-Nielsen, H., Lynch, K. A., Pfaff, R. F., Swaminathan, P. K., Kumar, C. K., Dogra, V. K., Stoyanov, B. J., Delamere, P. A., Bounds, S., and Gatsonis, N. A., "The APEX North Star Experiment: Observations of High-Speed Plasma Jets Injected Perpendicular to the Magnetic Field," *Advances in Space Research*, Vol. 29, No. 9, 2002, pp. 1317–1326.

[6]Podgorny, A. I., Podgorny, I. M., and Minami, S., "Numerical Simulation of the Artificial Plasma Jet in the Magnetosphere," *Advances in Space Research*, Vol. 24, No. 8, 1999, pp. 993–996.

[7]Podgorny, A. I., and Podgorny, I. M., "Dynamics of a Plasma Jet in the Magnetosphere in MHD Approximation, 2," *Cosmic Research*, Vol. 35, No. 3, 1997, pp. 236–244.

[8]Gavrilov, B. G., Erlandson, R. E., Kiselev, Y. N., Meng, C. I., Podgorny, I. M., Sobyanin, D. B., and Zetzer, J. I., "Dynamics of High Energy Plasma Jet in the Space. In Situ Experiment and Laboratory Simulation," *Advances in Space Research*, Vol. 21, No. 5, 1998, pp. 773–776.

[9]Sobyanin, D. B., Gavrilov, B. G., and Podgorny, I. M., "Laboratory Investigation of Plasma Jet Interaction with Transverse Magnetic Field," *Advances in Space Research*, Vol. 29, No. 9, 2002, pp. 1345–1349.

[10]Carlson, C. W., Curtis, D. W., Paschmann, G., and Michael, W., "An Instrument for Rapidly Measuring Plasma Distribution Functions with High Resolution," *Advances in Space Research*, Vol. 2, No. 5, 1983, pp. 67–70.

[11]Zetzer, J. I., Kozlov, S. I., Rybakov, V. A., Ponomarenko, A. V., Smirnova, N. V., Romanovsky, Yu. A., Meng, C. I., Erlandson, R. E., and Stoyanov, B. J., "Airglow in the Visible and Infrared Spectral Ranges of the Disturbed Upper Atmosphere Under Conditions of High-Velocity Plasma Jet Injection: I. Experimental Data," *Cosmic Research*, Vol. 40, No. 3, 2002, pp. 233–240.

[12]Pfaff, R. F., Freudenreich, H. T., Bounds, S., Delamere, P. A., Erlandson, R. E., Meng, C. I., Zetzer, J. I., and Gavrilov, B. G., "Electric Field, Magnetic Field, and Density Measurements on the Active Plasma Experiment," *Journal of Spacecraft and Rockets*, Vol. 41, No. 4, 2004, pp. 521–532.

D. L. Cooke
Guest Editor